Model Predictive Control of a Variable Speed Diesel Generator Interfaced to an AC Ship Power System as a Virtual Synchronous Machine

Magnus Jenssen[*]
[*]Department of Engineering Cybernetics
Norwegian University of Science and Technology
Trondheim, Norway

Jon Are Suul[*,#]
[#]SINTEF Energy Research
Trondheim, Norway
e-mail: jon.are.suul@ntnu.no, Jon.A.Suul@sintef.no

Abstract—This paper presents an adaptive implementation of model predictive control (MPC) for a variable speed diesel generator operated as a back-up energy source in an ac ship power system. The variable-speed operation is based on a diesel motor driving a synchronous machine (SM) with a diode rectifier and a boost converter as the interface to the dc-link of a voltage source converter (VSC) connected to the ac bus. The VSC is operated as a Virtual Synchronous Machine (VSM) for ensuring flexibility in supporting islanded operation of the ship power system at low load. The MPC strategy is designed for controlling the diesel generator torque and the excitation of the SM, and for regulating the dc-link voltage by providing a current reference for the boost converter. Adaptive operation of the MPC implementation is introduced by using a linearized prediction model updated at the operating conditions of each time-step. Simulation results demonstrate how the proposed implementation can ensure a more robust performance and a wider range of stability in response to large load variations in the ac bus than a conventional approach based on independent PI-controllers.

Index Terms—Model Predictive Control, Ship Power System, Variable Speed Diesel Generator, Virtual Synchronous Machine.

I. INTRODUCTION

Over the last decades, diesel-electric propulsion has become dominant for ships with large load variations or requirements for fast dynamic response [1], [2]. Traditionally, diesel-electric ship power systems have been based on ac distribution with Constant Speed Diesel Generators (CSDG). Thus, variable speed propulsion drives are typically interfaced to the ac bus by diode rectifiers or active front-end converters [1], [3].

Currently, applications of dc-distribution in ship power systems are developing quickly as the technology for dc grid protection is maturing [3], [4]. The individual interfacing of generators to a dc bus by passive or active rectifiers allows for variable speed operation to take advantage of the fuel efficiency characteristics of diesel motors [5], [6]. The recent developments towards utilization of on-board Li-ion battery storage systems are also favouring the use of dc distribution systems [3]. However, the majority of existing diesel-electric ship power systems are based on ac distribution. Thus, there is a significant potential for reducing emissions from vessels with ac power systems by retrofitting battery systems and introducing measures for increasing energy efficiency.

For long term operation at low loads, optimal loading of CS-DGs in a battery-hybrid ac system will imply intensive cycling of energy in the battery storage, which would compromise battery lifetime and the overall energy efficiency of the system. Alternatively, variable speed operation of a single generator could be a relevant option for reducing fuel consumption during low load conditions. However, operation of a Variable Speed Diesel Generator (VSDG) for supplying ac loads in stand-alone operation will require the converter interfaced to the ac bus to operate in grid forming mode [7]. Consequently, this configuration implies challenges for the control of both the DC/AC converter and the diesel generator.

This paper studies the control of a variable speed back-up diesel generator interfaced to an ac bus by a diode rectifier and a boost converter for controlling the dc-link voltage of a Voltage Source Converter (VSC). To enable flexible operation of the VSDG in both islanded mode and in parallel to traditional CSDGs, the ac-side converter will be controlled as a Virtual Synchronous Machine (VSM) [8]. In this system, the control of the governor and exciter of the generator as well as the dc voltage control by the boost converter will be of critical importance for ensuring power balance and stability in response to variations in the load on the ac bus. Thus, an adaptive implementation of Model Predictive Control (MPC) is proposed for providing the torque command for the diesel motor, the exciter voltage of the synchronous generator and the current reference for the boost converter. The performance of the proposed control strategy is bench-marked against a conventional control system design based on individual Proportional-Integral (PI) controllers for the governor, exciter and boost converter. Simulation results show that the presented MPC-based approach can ensure a wider range of stability in response to large load variations in the ac bus than the conventional PI-based control system.

II. STUDIED SYSTEM CONFIGURATION

A. System overview

The studied configuration with a variable speed back-up diesel generator implemented in a typical ac ship power system is shown in Fig. 1. The AC/DC/AC conversion stages for the variable speed generator consists of a six-pulse diode rectifier, a boost converter in continuous conduction mode with its
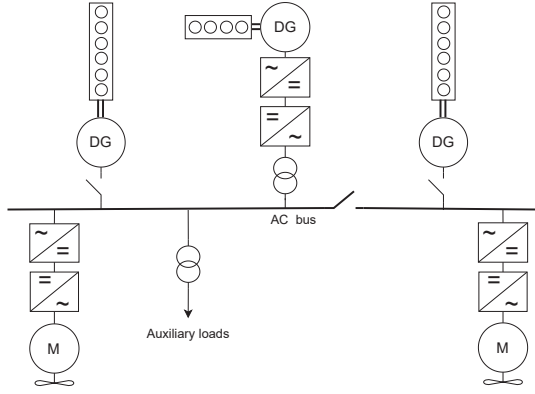
Fig. 1. Ship power system with variable speed back-up diesel generator for operation in low load conditions.
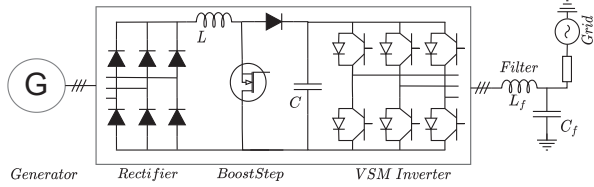

Fig. 2. The topology of the studied AC-DC-AC conversion system for variable-speed operation.
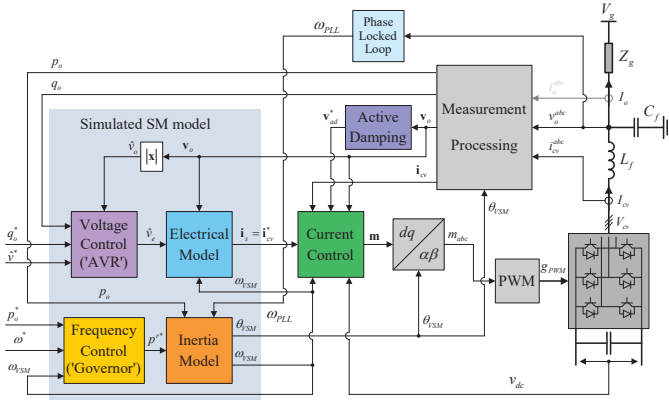

Fig. 3. Overview of VSM-based control of AC-side converter [8]

equivalent inductance, and a three-phase VSC between the dc-link and the ac bus [9], as shown in Fig. 2.

B. Control of the VSC interface to the ac bus

The VSC connected to the ac bus is controlled as a Virtual Synchronous Machine (VSM) [10], [11]. This ensures capability for handling both parallel operation with other generators and islanded operation, without any change in control structure or parameters. The applied VSM implementation uses a quasi-stationary electrical model to emulate the stator impedance of a Synchronous Machine (SM) and to provide the current references for an inner loop current controller [8]. Furthermore, a virtual swing equation is used to emulate the inertial dynamics of an SM. An overview of the VSM control system adapted from [8] is shown in Fig. 3.
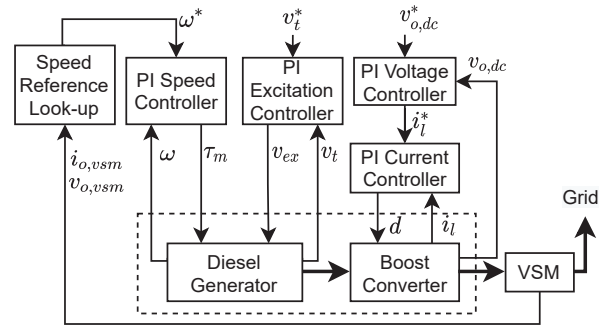

Fig. 4. Conventional PI-based control strategy for diesel generator and boost converter for dc-link voltage control.

C. Variable speed diesel generator

The main focus of this paper is on the generator-side control of the system, including the speed control (governor function), the terminal voltage control (exciter function) and the dc-link voltage control. The boost converter is used to control the dc-link voltage, since this decouples the SM terminal voltage from the dc-link voltage and relieves the exciter of the SM. This also provides an additional degree of freedom in control, as both the excitation and duty cycle of the boost converter can be used to control the dc-link voltage. The three aforementioned control paths (governor, exciter and converter) participates in the balance between electrical and mechanical power, which determines the acceleration of the generator shaft.

III. CONTROL SYSTEM DESIGN FOR VARIABLE SPEED DIESEL GENERATOR

A. Conventional PI-based control

A benchmark case with a conventional control system using three independent control paths designed as separate Single Input Single Output (SISO) controllers is shown in Fig. 4. The speed and excitation controllers are single loops, while the boost converter has cascaded inner and outer loop PI controllers for current and voltage, respectively. The conventional control system does not have any built-in mechanism to ensure balance between mechanical and electrical power. Thus, the electrical power could easily surpass the available mechanical power during low speed operation, which would cause the diesel engine to stall.

B. Speed reference look-up

In order to reduce fuel consumption by variable speed operation, a look-up table is introduced to adjust the generator speed reference ω^* in accordance with the load situation. An equivalent admittance, continuously calculated from the measured ac-side current $i_{o,vsm}$ and voltage $v_{o,vsm}$, is used as a measure of connected ac-side load. The calculated admittance is filtered through a backlash[1] and a low pass filter to remove signal noise, as shown in Fig. 5 [13]. Fig. 6 shows the relation between admittance and speed reference in the look-up table.

[1]The backlash locks the input signal at the instant of directional change until the signal has moved in the same direction for longer than the set threshold [12]. Thus, the backlash effectively removes signal noise.
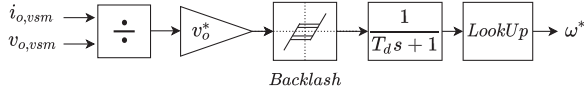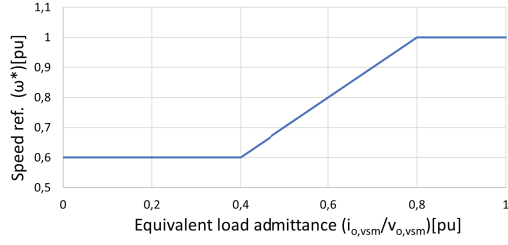
Fig. 5. Speed reference look-up method [13].

Fig. 6. Look-up table for generator speed reference.

Fig. 7. MPC-based control strategy for diesel generator and boost converter for dc-link voltage control.

C. Model Predictive Control

The Model Predictive Controller (MPC) illustrated in Fig. 7 inherently has a Multiple Input Multiple Output (MIMO) architecture, Thus, it uses all control inputs collectively in order to control the system outputs in accordance with a relative measure of importance. This is done by minimizing a finite horizon minimal value Quadratic Programming (QP) problem at each controller instant [14]. The QP problem cost function includes plant state errors, control inputs, control input rates ect. for every time step in the horizon, and thus, an optimal trajectory for the states and control inputs is found. The control input corresponding to the first time step in the calculated trajectory is applied to the plant [14].

The proposed MPC directly acts on the exciter voltage v_{ex} and the fuel injection signal (or mechanical torque signal τ_m in this simplified model), while it indirectly acts on the boost converter duty cycle d by providing the current reference i_l^* for an inner loop PI controller. The MPC can be expressed on standard form as:

$$J(z_k) = \sum_{i=0}^{p-1} \Big(\; [e_y^T(k+i)Qe_y(k+i)]$$
$$+ \; [e_u^T(k+i)R_u e_u(k+i)] \tag{1}$$
$$+ \; [\Delta u^T(k+1)R_{\Delta u}\Delta u(k+i)] \Big) \; + \; \rho_\epsilon \epsilon^2$$

where,

$$Q = \mathrm{diag}(0 \; \ldots \; 0 \; 30 \; 20 \; 60 \; 30 \; 20 \; 120) \tag{2a}$$
$$R_u = \mathrm{diag}(0 \; 0 \; 0) \tag{2b}$$
$$R_{\Delta u} = \mathrm{diag}(400 \; 200 \; 400) \tag{2c}$$
$$\tag{2d}$$

$$r = \begin{bmatrix} 0, & \ldots & v_t^* & \omega^*, & v_{o,dc}^*, & 0, & 0, & 0 \end{bmatrix}^T \tag{3a}$$
$$y = \begin{bmatrix} 0, & \ldots & v_t, & \omega, & v_{o,dc}, & \xi, & \rho, & \gamma \end{bmatrix}^T \tag{3b}$$
$$u = \begin{bmatrix} v_{ex}, & \tau_m, & i_l^* \end{bmatrix}^T \tag{3c}$$
$$u_{target} = \begin{bmatrix} 0 & 0 & 0 \end{bmatrix}^T \tag{3d}$$

$$e_y(k+i) = r(k+i+1) - y(k+i+1) \tag{4a}$$
$$e_u(k+i) = u_{target}(k+i) - u(k+i) \tag{4b}$$
$$\Delta u(k+i) = u(k+i) - u(k+i-1) \tag{4c}$$

As can be seen from (1)-(4), the MPC cost function consists of three penalized differences, where; *i)* e_y is the difference between the measured variables y and the references r, *ii)* e_u is the difference between the control inputs u and their respective targets u_{target}, and *iii)* Δu is the difference between control inputs $u(k+i)$ at step i in the horizon and the control inputs $u(k+i-1)$ at step $i-1$ in the horizon. The k operator indicates the controller instant while the i operator indicates the time step index in the horizon corresponding to the k-th controller instant. The term $\rho_\epsilon \epsilon^2$ is used to include slack variables in the cost function, in connection with the soft inequality constraints. A complete description of the generalized QP problem, subjected to linear inequalities and equality constraints, can be found in [15].

The MPC tuning is done through the cost function weighing matrices Q, R_u, $R_{\Delta u}$. The cost of error between measured variables y and references r is set in the matrix Q. The dc-link voltage $v_{o,dc}$ can be considered to be the most important variable in the MPC system, because it directly affects the maximal magnitude of the ac-side voltage. The VSDG speed ω and terminal voltage v_t are in this context secondary objectives where larger transient deviations can be allowed to assist the dc-link voltage reference tracking. Thus, the dc-link voltage $v_{o,dc}$ error has the highest cost setting in Q. Furthermore, the cost for deviation between control inputs u and their specific targets u_{target} is deactivated by setting R_u to zero, so that the control input usage does not contribute in the cost function. However, the rate of change on control inputs Δu is penalized through $R_{\Delta u}$. A large diagonal entry in $R_{\Delta u}$ makes the respective control input behave slower, which is comparable to a gain reduction in a conventional controller.

The upper and lower bounds in Table I are included as inequality constraints in the QP-problem. However, the exact mathematical description of the constraints are not included in this paper due to space limitations. The soft/hard setting indicates whether a low or high penalty (ρ_ϵ) is set on each respective inequality constraint slack variable (ϵ). The bounds

3

TABLE I
MPC BOUNDS

Variable	Lower	Upper	Variable type	Bound type
d	0.1	0.99	measured	soft
v_t	0	1.3	measured	soft
$v_{o,dc}$	0	∞	measured	soft
ω	0	1	measured	soft
v_{ex}	0	6	manipulated	hard
τ_m	0	1	manipulated	hard
i_l^*	0	3	manipulated	hard

on measured variables are made soft to avoid infeasible initial conditions during plant disturbances, e.g load variations. Note that the boost converter duty cycle d becomes a measured variable from the perspective of the MPC because it is controlled by the inner loop PI controller. The duty cycle is by definition limited between 0 and 1 and is for this reason logically saturated at the PI controller output. However, due to the numerical implementaiton, the MPC prediction model is not valid when the duty cycle approaches 0 or 1 [13]. The saturation in the PI controller is therefore set slightly above zero (0.01) and below one (0.99) in order to avoid feedback of these values to the MPC. A soft bound on duty cycle is also added in the MPC, as shown in Table I, in order to avoid operation in this area.

D. Prediction model

A linearized and discretized average model, including the generator, rectifier and boost converter, is implemented in the MPC QP problem as a linear equality constraint. The term "prediction model" is used in general when referring to this model in any of the three forms, being; non-linear form, linearized form or discretized form. The green area in Fig. 7 illustrates the scope of the prediction model.

A key remark regarding the applied prediction model is that the open loop power system is unstable, and therefore, the prediction model is unstable by definition. However, by adding some control on the fastest dynamics in the basic control layer, i.e. current controller, the fastest dynamic responses in the prediction model becomes slower, enabling the MPC to operate on a longer time scale. The rule according to [16] is that the prediction model step responses must be finite over the predicted time horizon (horizon length · time step) in order for the MPC calculations to be performed correctly. In other words, the time it takes for the fastest prediction model step response to become infinite, dictates the maximal length of prediction. When considering the slow dynamics in the power system, which is the mechanical inertia of the system, a long prediction horizon is needed in order to make accurate predictions. However, because the dc-current dynamic is much faster than the generator inertia, the step response would become infinite (from a computational point of view) during this long horizon if it was not for the inner loop controller.

The model components used to construct the full prediction model are presented i the following. Specifically, the voltage balance equations for the direct and quadrature axes of the stator windings and for the field winding are used to represent

the electrical dynamics of the SM in rotating (dq) reference frame, as given by [17]:

$$v_d = -r_s i_d - \frac{x_d}{\omega_b}\frac{di_d}{dt} + \frac{x_{ad}}{\omega_b}\frac{di_f}{dt} + \omega_r x_q i_q \tag{5a}$$

$$v_q = -r_s i_q - \frac{x_q}{\omega_b}\frac{di_q}{dt} + \omega_r\left(-x_d i_d + x_{ad} i_f\right) \tag{5b}$$

$$v_f = r_f i_f - \frac{x_{ad}}{\omega_b}\frac{di_d}{dt} + \frac{x_f}{\omega_b}\frac{di_f}{dt} \tag{5c}$$

The shaft acceleration is given by the first order swing equation (6), where $\tau_m\omega$ is the mechanical power, p_e is the electrical power and H is the inertia constant of the SM.

$$\frac{d\omega}{dt} = \frac{\tau_m\omega - p_e}{2H} \tag{6}$$

The engine torque τ_m is assumed to be proportional to the fuel command and is therefore utilized directly as a control input to the system.

The delay in the excitation system, between the exciter voltage signal v_{ex} and the field winding voltage v_f is approximated by a low pass filter as:

$$\frac{dv_f}{dt} = \frac{r_f}{x_{ad}}\frac{v_{ex}}{T_{ex}} - \frac{v_f}{T_{ex}} \tag{7}$$

The factor r_f/x_{ad} converts the exciter voltage from the excitation system per unit representation to the per unit system of the stator windings. Consequently, the excitation control signal v_{ex} has a scaling more practical for the excitation system where unity voltage yields unity current in the field winding. This is in contrast to the per unit system referred to the stator windings, which is defined from the no-load condition and results in a very small field voltage base quantity. This method of conversion between per unit systems is more thoroughly described in [18].

A continuous conduction mode (CCM) average model as given by (8) is used to describe the boost circuit including the equivalent parasitic resistance r_l of the boost inductance l_{boost}. The boost converter model consists of the inductance current i_l state and the the dc output voltage $v_{o,dc}$ state.

$$\frac{di_l}{dt} = \frac{\omega_b}{l}\left(v_{s,dc} - r_l i_l - (1-d)v_{o,dc}\right) \tag{8a}$$

$$\frac{dv_{o,dc}}{dt} = \frac{\omega_b}{c}\left((1-d)i_l - \frac{v_{o,dc}}{|z_o|}\right) \tag{8b}$$

The AC-side interface is not included in the prediction model but is instead interfaced through the equivalent impedance z_o acting as a disturbance input to the MPC prediction model.

As already indicated, the current controller forms a basic control layer and is therefore included in the prediction model as:

$$d = k_{pi}(i_l^* - i_l) + k_{ii}\zeta \tag{9a}$$

$$\frac{d\zeta}{dt} = i_l^* - i_l \tag{9b}$$

The algebraic relation from the SM (5) to the boost converter (8) is made through the dc input voltage $v_{s,dc}$ as:
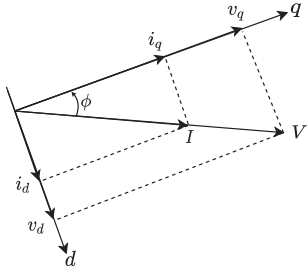
$$v_{s,dc} = \sqrt{v_d^2 + v_q^2} - \Delta v_s \tag{10}$$

Fig. 8. Voltage and current phasors at the generator terminals with the assumption of unity power factor.

Fig. 9. Implementation principles of adaptive linear MPC.

Here, the voltage drop due to commutation, Δv_s, in the three phase six-pulse diode rectifier is given by [9]:

$$\Delta v_s = \frac{3l_{boost}}{2\pi}\omega I \qquad (11)$$

The boost converter inductance l_{boost} is assumed to be given from the SM sub-transient armature winding inductances as:

$$l_{boost} = \sqrt{l_d''^2 + l_q''^2} \qquad (12)$$

The phase angle between current and voltage at the generator terminals is assumed to be zero, as shown in Fig. 8. This enables a simple algebraic relation as given by (13) between the boost converter equations (8) and the electrical model of the generator (5).

$$v_d = V\frac{i_d}{I} \qquad (13a)$$

$$v_q = V\frac{i_q}{I} \qquad (13b)$$

$$p_e = s_e = IV \qquad (13c)$$

$$I = i_l \qquad (13d)$$

$$V = (1 - d)v_{o,dc} + \Delta v_s \qquad (13e)$$

Using the modelling shown in equations (5) through (13), an 8$^{\text{th}}$ order explicit non-linear state space model can be formed. Additionally, four states was included in the model for technical and control purposes. Firstly, a low pass filter (14) was included in series with the current reference i_l^* to avoid direct feedthrough form inputs to outputs in the prediction model (which is not allowed in the Matlab MPC toolbox).

$$\frac{di_{l,2}^*}{dt} = \frac{i_l^* - i_{l,2}^*}{T_t} \qquad (14)$$

Secondly, the three states in (15) were included in the prediction model to equip the MPC with integral action. Penalizing the integrated error on the measured variables v_t, ω and $v_{o,dc}$ greatly improved the controller performance with respect to reference tracking.

$$\frac{d\xi}{dt} = v_t^* - \sqrt{v_d^2 + v_q^2} \qquad (15a)$$

$$\frac{d\rho}{dt} = \omega^* - \omega \qquad (15b)$$

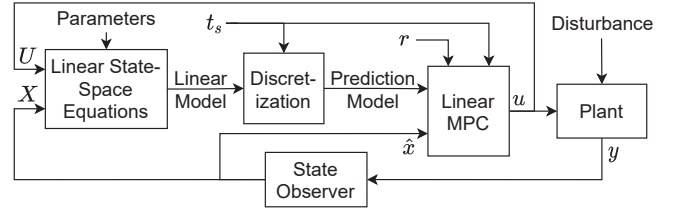$$\frac{d\gamma}{dt} = v_{o,dc}^* - v_{o,dc} \qquad (15c)$$

TABLE II
POWER SYSTEM SIMULATION

Symbol	Expression	Description
V_{ph}	398.37	Rated phase RMS voltage [V]
I_n	740.54	Rated line current [A]
S_b	885.0	Rated apparent power [kVA]
f_b	60	Rated frequency [Hz]
p_{vsm}^*	0.4	Active power reference VSM [pu]
p_{vsdg}^*	0.28 or 0.2	Active power reference VSDG [pu]

E. Adaptive MPC

The non-linear prediction model must be linearized around an operating point in order to be implemented as a linear equality constraint in the MPC QP problem. However, because the variable speed generator system is highly nonlinear, the linear prediction model cannot provide the required accuracy during operation away form the operating point. The linear MPC is therefore implemented with adaptive functionality where the prediction model operating point is updated according to the plant measurements at every controller iteration [13], [19]. The principles applied for implementing the adaptive MPC are illustrated in Fig. 9.

The jacobian matrices for the linearized model are not presented here due to space constraints. However, the explicit form of the complete prediction model was constructed and linearized by the use of the Matlab symbolic toolbox.
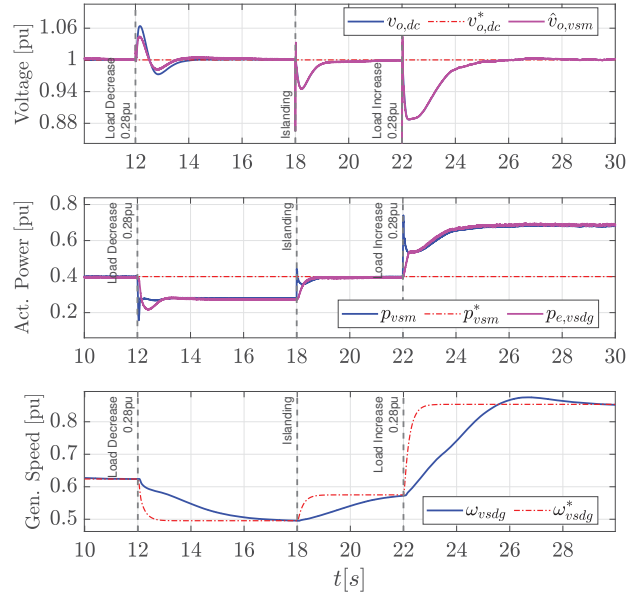
IV. SIMULATION RESULTS

For evaluating the performance of the studied control strategies, a numerical power system simulation is performed. The power system parameters used in the simulation are provided in Table II. One single CSDG is initially assumed to be online in addition to the VSDG. Two resistive loads are first shared between the CSDG and the VSDG. The simulated power system is subjected to three disturbances. During simulation, one of the two loads is disconnected at t = 12 s, before the constant speed generator is turned off at t = 18 s and the same load is then again connected at t = 22 s.

Note that the active power reference p_{vsdg}^* for the VSDG is set to be equal to the load variation in each case. As the active power references for the VSM and CSDG are constants in the simulations, the delivered power will not be kept at the reference but will vary with the load situation. However, the power unit with the highest power reference will supply most of the load power.

The first event (load decrease) serves as an indication of the dynamic response with both power sources connected to
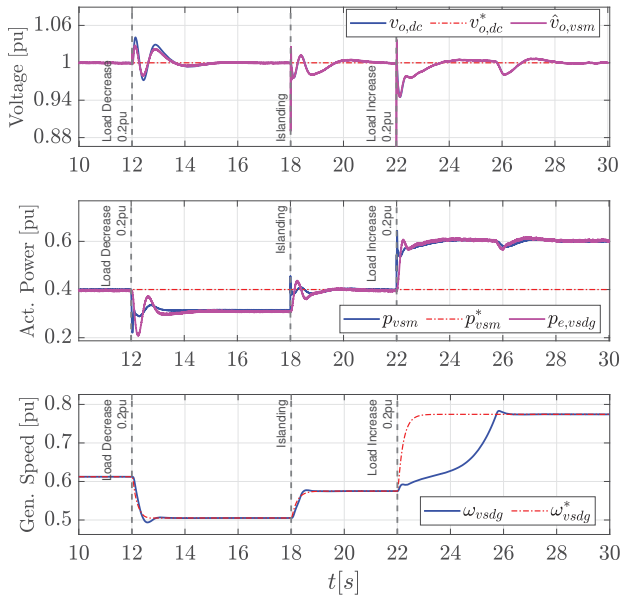
5
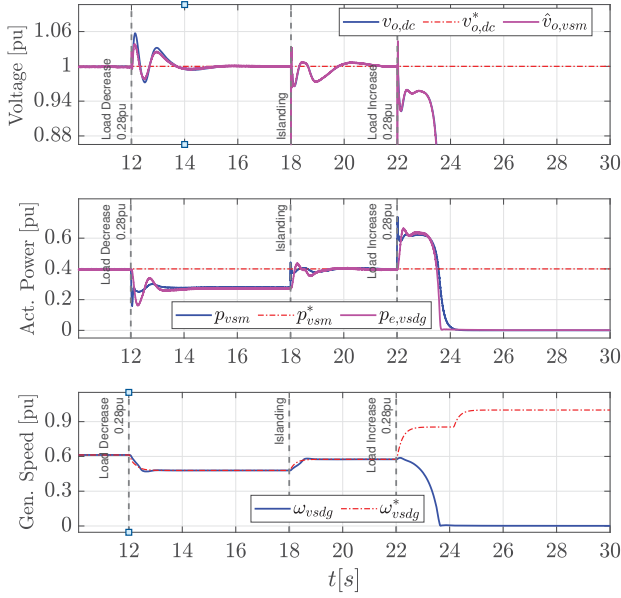
(a) Conventional PI-based control

(b) MPC-based control

Fig. 10. Simulation results demonstrating the MPC's ability to maintain power balance and system stability during load increase.

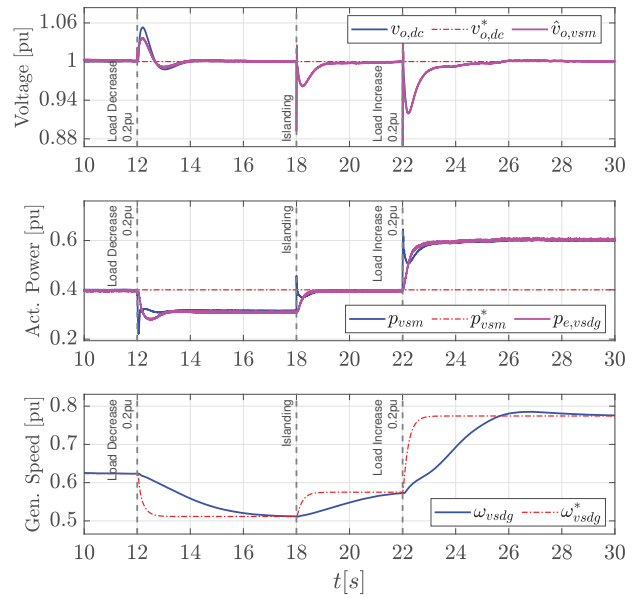(a) Conventional PI-based control

(b) MPC-based control

Fig. 11. Simulation results demonstrating the MPC's ability to maintain power balance and system stability during load increase.

the same ac grid. As the load power is reduced from 0.6 pu to 0.4 pu, the power delivered by the VSDG decreases by 0.1 pu while the CSDG power also decreases 0.1 pu. To limit the amount of presented data, only the VSDG and VSM variables are shown in Fig. 10 and 11.

During the second event (islanding) at t = 18s, the load power remains unchanged, but all power delivered from the

CSDG is shifted to the VSDG as the CSDG goes offline.

The last, and possibly most interesting, event is the load increase occurring at t = 22s. Here, the same load is again connected while the VSDG operates as in islanded mode. The comparison between the two control systems is performed with two different load variations. In Fig. 11 the load increase during islanded operation is sufficiently low (0.2 pu) for the

6

conventional control system to remain stable. However, with the larger load increase (0.28 pu) in Fig. 10, the conventional control system becomes unstable as the electrical power ($>$0.6 pu) exceeds the mechanical power capability at the operating speed (0.6 pu). On the other hand, the MPC-based approach handles both levels of load increase by limiting the electrical power delivered to the load through a momentary voltage decrease, so that the generator is allowed to accelerate.

A few remarks on the presented simulation results is given in the following:

- In all cases, a difference can be seen in the transient behavior between the VSDG and the VSM power and voltage. This transient difference is a result of the power flow in and out of the dc-link capacitor after a change in load power.
- There is clearly a difference in the overall behavior between the conventional SISO-based control and MPC-based control. The MPC allows for a "looser" speed reference tracking than the conventional because the MPC cost function is tuned to prioritize voltage control over speed control.
- It is also evident that the voltage control is, unintentionally, affected by the speed control in the conventional control system. Thus, a disturbance can be seen in the voltage at the moment when the torque input τ_m decreases as the speed reaches the reference (see Fig. 11(a) at t = 25.7s).

In all cases, the look-up table in Fig. 6 provides the speed reference. The look-up table should be adjusted to meet the requirement for spinning reserve in accordance with the expected load variations and the grid side tolerances for voltage quality. To ensure stability of the conventional control system during load surges, the speed reference look-up table must be set conservatively such that there is a large spinning reserve present for each load level. In other terms, the conventional control system can only function when the system is operated well within the physical limit of the mechanical system. The lack of power balancing mechanisms in the conventional control system may limit the potential for optimizing the operation with respect to fuel saving.

V. Conclusion

This paper has proposed a linear adaptive MPC control scheme for a VSDG connected to an AC grid through a diode rectifier, a controlled boost converter and a VSM. An MPC prediction model was constructed by the use of classical SM modelling and average models of the power electronic conversion stages. The MPC-based control was compared to a classical control system based on conventional PI controllers, by the use numerical power system simulations. The MPC-based approach was shown capable of maintaining power balance in the system. This, it can expand the range of operation and sustain system stability closer to the physical stability limit than what was achieved when using the conventional approach.

Further work for improving the proposed control strategy would imply a closer evaluation of the real time implementation. The MPC control topology would then have to be considered with respect to the available computational resources. In this context, it may be a good idea to go from the single MPC structure presented in this paper, to a cascaded structure, with an inner loop MPC for the fast dynamics and an outer loop MPC for the slower dynamics. A time scale separation between inner and outer loop, might allow for a much shorter prediction horizon to be used in the inner and outer loops, and thus, lowering the computational effort. It would also be interesting to do a performance comparison between the linear adaptive MPC and a non-linear MPC.

References

[1] J. F. Hansen and F. Wendt, "History and state of the art in commercial electric ship propulsion, integrated power systems, and future trends," *Proceedings of the IEEE*, vol. 103, no. 12, pp. 2229–2242, 2015.

[2] D. Paul, "A history of electric ship propulsion systems [history]," *IEEE Industry Applications Magazine*, vol. 26, no. 6, pp. 9–19, 2020.

[3] E. Skjong, R. Volden, E. Rødskar, M. Molinas, T. A. Johansen, and J. Cunningham, "Past, present, and future challenges of the marine vessel's electrical power system," *IEEE Transactions on Transportation Electrification*, vol. 2, no. 4, pp. 522–537, 2016.

[4] G. Sulligoi, A. Vicenzutti, and R. Menis, "All-electric ship design: From electrical propulsion to integrated electrical and electronic power systems," *IEEE Transactions on transportation electrification*, vol. 2, no. 4, pp. 507–521, 2016.

[5] O. Mo and G. Guidi, "Design of minimum fuel consumption energy management strategy for hybrid marine vessels with multiple diesel engine generators and energy storage," in *2018 IEEE Transportation Electrification Conference and Expo (ITEC)*, 2018, pp. 537–544.

[6] J. F. Hansen, F. Wendt, and J. O. Lindtjørn, "Fuel efficient power plant featuring variable speed generation system for dp drilling units," in *Proc. Dyn. Positioning Conf.*, 2016, pp. 1–13.

[7] J. Rocabert, A. Luna, F. Blaabjerg, and P. Rodriguez, "Control of power converters in ac microgrids," *IEEE transactions on power electronics*, vol. 27, no. 11, pp. 4734–4749, 2012.

[8] O. Mo, S. D'Arco, and J. A. Suul, "Evaluation of virtual synchronous machines with dynamic or quasi-stationary machine models," *IEEE transactions on industrial electronics (1982)*, vol. 64, no. 7, pp. 5952–5962, 2017.

[9] N. Mohan, "Power electronics : converters, applications, and design," New York, 1995.

[10] H.-P. Beck and R. Hesse, "Virtual synchronous machine," in *2007 9th International Conference on Electrical Power Quality and Utilisation*. IEEE, 2007, pp. 1–6.

[11] S. D'Arco and J. A. Suul, "Virtual synchronous machines—classification of implementations and analysis of equivalence to droop controllers for microgrids," in *2013 IEEE Grenoble Conference*. IEEE, 2013, pp. 1–7.

[12] MathWorks. Backlash. https://www.mathworks.com/help/simulink/slref/backlash.html, (visited on 12/09/2021).

[13] M. Jenssen, "Model predictive control of a variable speed back-up diesel generator interfaced to an ac ship power system as a virtual synchronous machine," Master's thesis, Department of Engineering Cybernetics NTNU, Trondheim, Norway, 2021.

[14] B. Foss and T. A. N. Heirung, "Merging optimization and control," *Lecture Notes*, 2013.

[15] MathWorks. Optimization problem. https://www.mathworks.com/help/mpc/ug/optimization-problem.html, (visited on 18/04/2021).

[16] ——. Choose sample time and horizons. https://www.mathworks.com/help/mpc/ug/choosing-sample-time-and-horizons.html, (visited on 05/05/2021).

[17] J. Machowski, J. Bumby, J. W. Bialek, and D. J. Bumby, *Power System Dynamics: Stability and Control*. New York: John Wiley & Sons, Incorporated, 2008.

[18] J. A. Suul, "Control of variable speed pumped storage hydro power plant for increased utilization of wind energy in an isolated grid," Master's thesis, Department of Electrical Power Engineering NTNU, Trondheim, Norway, 2006.

[19] MathWorks. Adaptive mpc. https://www.mathworks.com/help/mpc/ug/adaptive-mpc.html, (visited on 30/06/2021).